

# CALCULATIONS OF THE GEODESIC CURVATURE OF A MAGNETIC LINE FOR THE URAGAN-2M TORSATRON WITH TAKING INTO ACCOUNT THE INFLUENCE OF THE CURRENT-FEEDS AND DETACHABLE JOINTS OF THE HELICAL WINDING

*V.V. Nemov, V.N. Kalyuzhnyj, S.V. Kasilov, G.G. Lesnyakov, N.T. Besedin\**  
*Institute of Plasma Physics, National Science Center "Kharkov Institute of Physics and Technology",  
Akademicheskaya Str. 1, 61108 Kharkov, Ukraine*

*\*Kursk State Technical University, 50 Let Oktyabrya str. 94, 305040 Kursk, Russia*

The database for the coils of the U-2M magnetic system which was formerly used in computations of magnetic surfaces with taking into account the influence of the current-feeds and detachable joints of the helical winding is transformed to a new form which is valid for the already existing Biot-Savart code for computations of the magnetic field strength, and its spatial derivatives. With this code, using the transformed database, computations are performed for the geodesic curvature of the magnetic field lines for few configurations of U-2M. These computations are considered as a preliminary work for future transport computations.

PACS: 52.55.Hc

## INTRODUCTION

Among big number of computational works related to a study of the magnetic field of the Uragan-2M (U-2M) torsatron an important place belongs to computations of magnetic surfaces with taking into account the influence of the current-feeds and detachable joints of the helical winding [1], [2]. The magnetic surfaces found as a result of such computations are the closest to real magnetic surfaces of the device. The numerical code used in the quoted works computes the magnetic field strength,  $B$ , from all elements of the helical winding using the Biot-Savart law. This is sufficient for the computation of the magnetic field lines as well as magnetic surfaces. At the same time, computations of many other confinement characteristics (e.g., transport processes, charged particle drift, etc.) are accompanied with computations of spatial derivatives of  $B$ , and a possibility to compute these quantities should be realized in the corresponding codes.

In this respect, the following study is carried out in the presented work. The database for the coils of the U-2M magnetic system used in computations of [1], [2] is transformed to a new form, which is valid for the already existing code for computations of  $B$  and its spatial derivatives. With this code, using the transformed data-base, computations of the magnetic surfaces are made for several sets of parameters of the magnetic system. Also, computations of the geodesic curvature of magnetic field lines,  $k_G$  are performed for few configurations of U-2M. Computation of this quantity is a necessary step in further computations of transport processes and charged particle drift for stellarator configurations.

## COMPUTATION OF MAGNETIC SURFACES

In a model of the magnetic system of U-2M used in Refs. [1], [2] the helical winding is split into a set of filamentary conductors. Additionally, each of the filaments is split into 200 short straight conductors. The Biot-Savart law is used for calculating the magnetic field of every such an element. By the analogous way, the magnetic field of the current feeds and the detachable joints is calculated. Now, the currents and the coordinates of the above mentioned straight elements calculated by the code of Refs. [1], [2] are written into a special data file of a standard form which is often used in calculations of the magnetic field of various stellarator devices

(see, e.g., in Ref. [3]). Such a new database can be conveniently used for the data input into the already existing code for computations of  $B$  and its spatial derivatives. With this code, using the new database, computations of the magnetic surfaces are made for the sets of parameters of the magnetic system corresponding to  $k_\phi=0.31$  and  $k_\phi=0.295$ , where  $k_\phi$  is connected with the toroidal components of the magnetic field produced by the helical winding,  $B_{th}$ , and the toroidal field coils,  $B_u$ , respectively,  $k_\phi = B_{th} / (B_u + B_{th})$ . Note that the magnetic field and its spatial derivatives from the toroidal field coils as well as the poloidal field coils are calculated using the complete elliptical integrals (as it has been done for the magnetic field in Refs [1], [2]).

Integration of the magnetic field lines is performed for the intervals corresponding to 250 (or even more) turns around the major axis of the torus. Cross-sections of the magnetic surfaces obtained as the results of these computations are presented in Figs. 1 and 2. These cross-sections as well as the rotational transform,  $\iota$ , are in good agreement with the corresponding results of Ref. [2]. It is seen from the figures that major parts of the magnetic configurations inside the vacuum chamber have regular magnetic surfaces. For  $k_\phi=0.295$ , island surfaces of moderate sizes corresponding to  $\iota = 1/3$  are seen in Fig. 1. For  $k_\phi=0.31$ ,  $\iota$  is within the limits  $1/3 < \iota < 1/2$  and islands corresponding to  $\iota = 2/5$  are also present in Fig. 2. Magnetic surfaces numbered in the figures are those for which the geodesic curvature of the field lines is calculated in the next section.

## COMPUTATION OF $k_G$ FOR U-2M

Computation of the geodesic curvature of a magnetic field line

$$k_G = \frac{(B \times \nabla B) \cdot \nabla \psi}{|\nabla \psi| B^2} \quad (1)$$

is an important step in transport computations and computations of charged particle drift (see, e.g., Refs. [4], [5]). The  $\psi$  quantity in (1) is the magnetic surfaces label. The  $\nabla \psi$  vector (which is normal to the magnetic surface) is calculated using a field line following code. Because of the non-symmetric arrangement of the current feeds and detachable joints the stellarator symmetry of the resulting magnetic field of U-2M is violated and there are no cross-sections of the magnetic surfaces with an up-down symmetry.

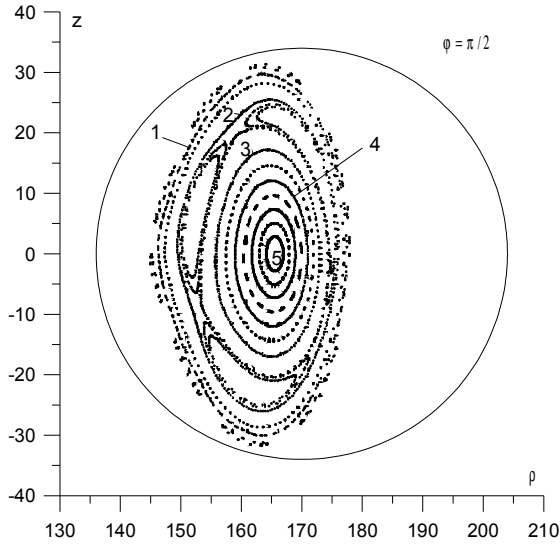


Fig.1. Magnetic surfaces of U-2M for  $k_\phi = 0.295$  inside the vacuum chamber. A circle with a radius of 34 cm shows an inner boundary of the vacuum chamber. Island surfaces that correspond to  $l = 1/3$  are seen at moderate distance from the magnetic axis. Small scale islands of  $l = 3/8$  are present not far from the vacuum chamber

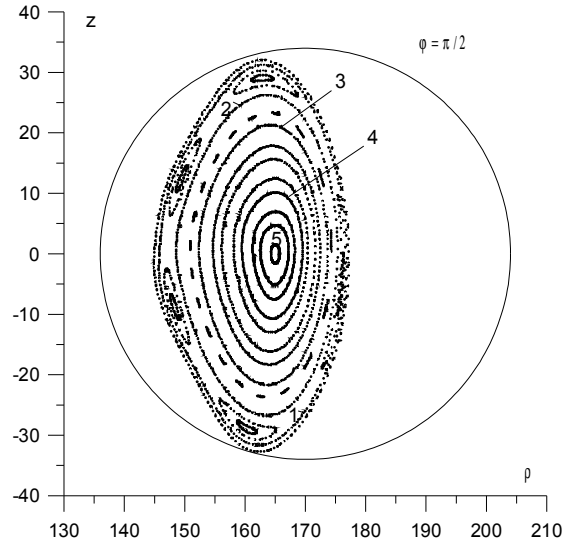


Fig.2. The same as in Fig.1 for  $k_\phi = 0.31$ . Island surfaces corresponding to  $l = 2/5$  are present not far from the vacuum chamber

This complicates a determination of starting conditions that are necessary for the further computation of using the integration along the magnetic field line. Now, a preliminary computation of the corresponding magnetic surface is necessary to find these conditions. After their determination, the consequent calculation of  $\nabla\psi$  is performed using an approach of Ref. [6] that is based on simultaneous integration of close magnetic field lines. This differs from the  $\nabla\psi$  calculations in Refs. [4] and [5] where the differential equations for  $\nabla\psi$  are solved and where the starting values of  $\nabla\psi$ ,  $(\nabla\psi)_0$ , are easily determined with high accuracy due to the presence of magnetic surface cross-sections with the up-down symmetry. The approach [6] is less sensitive to possible inaccuracy in the starting conditions that can take place because of the lack of the magnetic surface cross-sections with the up-down symmetry.

According to this approach  $\nabla\psi$  can be represented as

$$\nabla\psi = - \lim_{r_2(\varphi_0) \rightarrow r_1(\varphi_0)} \frac{(r_2(\varphi) - r_1(\varphi)) \times B}{((r_2(\varphi_0) - r_1(\varphi_0)) \times B(\varphi_0))} \quad (2)$$

Here, in the cylindrical coordinates  $\rho, \varphi, z$  the curves  $r_1(\varphi)$  and  $r_2(\varphi)$  satisfy the field line equations  $dr/d\varphi = \rho B/B_\varphi$  with starting points  $r_1(\varphi_0)$  and  $r_2(\varphi_0)$ , respectively, which are on the same magnetic surface and on the same meridian plane  $\varphi_0$ ;  $B(\varphi_0)$  is  $B$  for the starting point  $r_1(\varphi_0)$ . Such a representation of  $\nabla\psi$  corresponds to  $|\nabla\psi| = 1$  for the starting point.

Following Ref. [6], to explain formula (2), let us consider in coordinates  $\psi, \theta_0, \varphi$ , the infinitesimal distance,  $dr$

$$dr = e_1 d\psi + e_2 d\theta_0 + e_3 d\varphi \quad (3)$$

with

$$\begin{aligned} \vec{e}_1 &= \sqrt{g} (\nabla\theta_0 \times \nabla\varphi), \vec{e}_2 = \sqrt{g} (\nabla\varphi \times \nabla\psi), \\ \vec{e}_3 &= \sqrt{g} (\nabla\psi \times \nabla\theta_0), \sqrt{g} = 1/|(\nabla\psi \times \nabla\theta_0) \cdot \nabla\varphi| \end{aligned} \quad (4)$$

and  $\theta_0$  being an angle-like variable which labels a field line on a magnetic surface and satisfies the Clebsch representation of the magnetic field strength,

$$B = \nabla\psi \times \nabla\theta_0. \quad (5)$$

From (4) and (5) one finds

$$\nabla\psi = e_2 \times B, \quad (6)$$

To calculate  $e_2$  let us consider a particular value of  $dr$  from (3),  $dr$ , which corresponds to fixed  $\psi$  and  $\varphi$

$$dr_{\psi_0} = e_2 d\theta_0. \quad (7)$$

Since  $dr$  corresponds to  $r_2(\varphi) - r_1(\varphi)$  one obtains (2) from (6) and (7).

In the preliminary computation of any magnetic surface under consideration, integration of the magnetic field line was performed for a starting point  $r_1(\varphi_0)$  for an interval corresponding to 250 turns round axis. A Poincare plot for this field line was made in the  $\varphi_0$  plane and the nearest to  $r_1(\varphi_0)$  point of this plot was taken as a point  $r_2(\varphi_0)$ . After this, new simultaneous field line tracing computation of two field lines was performed with starting points  $r_1(\varphi_0)$  and  $r_2(\varphi_0)$ . With this,  $\nabla\psi$  and  $k_G$  were calculated using formulae (2) and (1), respectively.

The computational results for  $k_G$  are presented in a normalized form in Figs. 3 and 4 for non-island magnetic surfaces. These figures show the quantity  $Rk_G$  as a function of  $\gamma$  at the magnetic surface cross-sections  $\varphi = \varphi_0$ . Here,  $R$  is the major radius of torus and quantity  $\gamma$  is defined as  $\gamma = \vartheta/(2\pi)$ , where  $\vartheta$  is the angle which is counted around the center of the cross-section of each magnetic surface from the direction of the normal to the circular axis of the torus. From the benchmarking of the obtained results with the analogous results for the case where current-feeds and detachable joints are ignored one can conclude that these elements of the helical winding do not affect strongly the distributions of  $k_G$  over U-2M magnetic surfaces. Therefore, for non-island magnetic surfaces, one can expect that neoclassical transport coefficients for the case where the current-feeds and the detachable joints are taken into account will not differ strongly from those corresponding to the case

where these elements of the helical winding are ignored. However, more detailed study of this question is necessary to make confident conclusions.

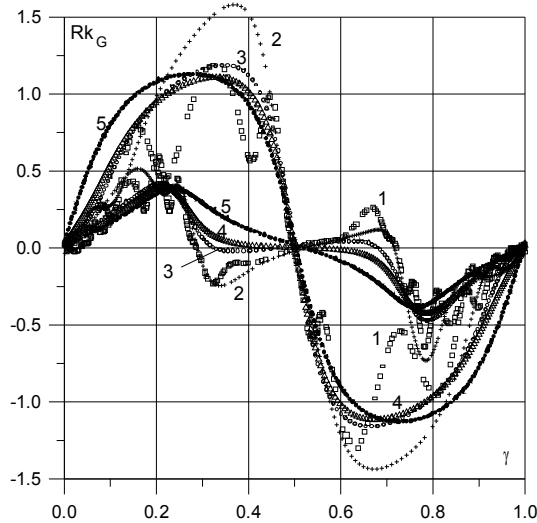


Fig.3. Normalized quantity  $k_G$  as function of  $\gamma$  in the case of  $k_\phi = 0.295$  for various magnetic surfaces. The plots 1 (squares), 2 (crosses), 3 (open circles), 4 (triangles) and 5 (thick points) relate to the magnetic surfaces of corresponding numbers in numbers in Fig.1. The curves with small amplitudes correspond to  $\varphi = \pi/2$  cross-section (vertically elongated), the curves with bigger amplitudes correspond to  $\varphi = \pi/4$  cross-section (horizontally elongated)

### CONCLUSIONS

To check the validity of the new database, computations of the magnetic surfaces of U-2M are performed. The results are found to be in good agreement with the corresponding results of Ref. [2]. An important consequence of the presence of current-feeds and detachable joints is that the stellarator symmetry of the magnetic field of U-2M is violated and there are no resulting cross-sections of the magnetic surfaces with an up-down symmetry. This fact essentially complicates the computation of the  $k_G$  quantity since in this case a preliminary computation of the magnetic surfaces should be performed to find the necessary starting conditions for further integration along the magnetic field lines.

### РАСЧЕТЫ ГЕОДЕЗИЧЕСКОЙ КРИВИЗНЫ СИЛОВЫХ МАГНИТНЫХ ЛИНИЙ ДЛЯ ТОРСАТРОНА УРАГАН-2М ПРИ УЧЕТЕ ВЛИЯНИЯ ТОКОПОДВОДОВ И ТОКОРАЗЪЕМОВ ВИНТОВОЙ ОБМОТКИ

*В.В. Немов, В.Н. Калюжный, С.В. Касилов, Г.Г. Лесняков, Н.Т. Беседин*

База данных для проводников магнитной системы торсатрона У-2М, использовавшаяся ранее для вычисления магнитных поверхностей с учетом влияния токоподводов и токоразъемов, преобразована к новому виду, который может использоваться в уже существующем коде на основе закона Био-Савара для вычисления напряженности магнитного поля и ее пространственных производных. С использованием этого кода и преобразованной базы данных выполнены расчеты геодезической кривизны силовых магнитных линий для нескольких конфигураций У-2М. Эти расчеты являются предварительным этапом последующих расчетов процессов переноса.

### РОЗРАХУНКИ ГЕОДЕЗИЧНОЇ КРИВИЗНИ СИЛОВИХ МАГНІТНИХ ЛІНІЙ ДЛЯ ТОРСАТРОНА УРАГАН-2М З УРАХУВАННЯМ ВПЛИВУ СТРУМОПІДВОДІВ ТА СТРУМОРОЗНІМАНЬ ГВИНТОВОЇ ОБМОТКИ

*В.В. Немов, В.М. Калюжний, С.В. Касилов, Г.Г. Лесняков, М.Т. Беседин*

База даних для провідників магнітної системи торсатрона У-2М, що використовувалася раніше для розрахунків магнітних поверхонь із урахуванням впливу струмопідводів та струморознімачів, перетворена до нового виду, який може використовуватися у вже існуючому коді на основі закону Біо-Савара для розрахунків напруженості магнітного поля та її просторових похідних. З використанням цього коду та перетвореної бази даних виконано розрахунки геодезичної кривизни силових магнітних ліній для декількох конфігурацій У-2М. Ці розрахунки є попереднім етапом наступних розрахунків процесів переносу.

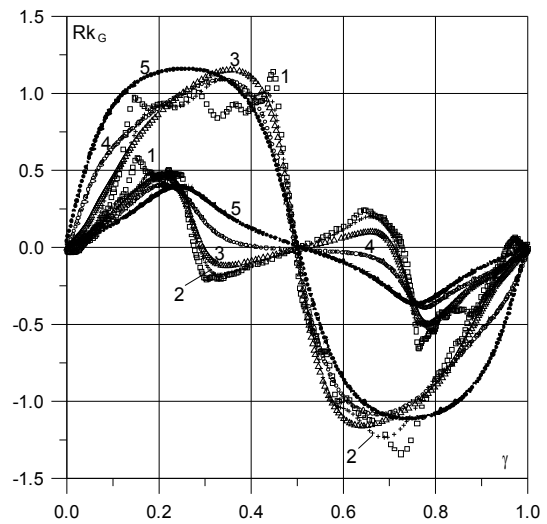


Fig.4. The same as in Fig.3 for  $k_\phi = 0.31$

Calculated values of  $k_G$  turn out to be not strongly different from the case where the influence of current-feeds and detachable joints is ignored. Therefore, one can expect that for the case where current-feeds and detachable joints are taken into account the neoclassical transport coefficients will not differ strongly from those corresponding to the case where these elements of the helical winding are ignored. A more detailed study of this question is necessary in future to make confident conclusions.

### REFERENCES

1. N.T. Besedin, G.G. Lesnyakov, I.M. Pankratov // *Voprosy Atomnoj Nauki i Tekhn. Ser. "Termoyadern. Sintez"*. 1991, №1, p.48 (in Russian).
2. G.G. Lesnyakov et al. // *Proceedings of the 23rd EPS Conf. on Contr. Fusion and Plasma Phys., Kiev, Ukraine, 24-28 June, 1996*, v.20 C, Part II, p.547 (Report b025).
3. M. Drevlak // *Fusion Technology*. 1998, v.33, p.106.
4. V.V. Nemov, S.V. Kasilov, W. Kernbichler, and M.F. Heyn // *Phys. Plasmas*. 1999, v.6, p.4622.
5. V.V. Nemov, S.V. Kasilov, W. Kernbichler and G.O. Leitold // *Phys. Plasmas*. 2005, v.12, p.112507.
6. H.L. Berk, M.N. Rosenbluth, J.L. Shohet // *Phys. Fluids*. 1983, v.26, p.2616.